

ENERGETIC PARTICLE INDUCED DESORPTION OF WATER VAPOR

CRYO-CONDENSATE *

CONF-901035--7

DE91 001255

M. M. Menon, L. W. Owen, J. E. Simpkins, T. Uckan, and P. K. Mioduszewski,
Oak Ridge National Laboratory, Oak Ridge, TN. 37831-8072

An in-vessel cryo-condensation pump is being designed for the Advanced Divertor configuration of the DIII-D tokamak. To assess the importance of possible desorption of water vapor from the cryogenic surfaces of the pump due to impingement of energetic particles from the plasma, a 77 K surface on which a thin layer of water vapor was condensed was exposed to a tenuous plasma (density = $2 \times 10^{10} \text{ cm}^{-3}$, electron temperature = 3 eV). Significant desorption of the condensate occurred, suggesting that impingement of energetic particles (10 eV) at flux levels of $\sim 10^{16} \text{ cm}^2 \text{ s}^{-1}$ on cryogenic surfaces could potentially induce impurity problems in the tokamak plasma. A pumping configuration is presented in which this problem is minimized without sacrificing the pumping speed.

1. INTRODUCTION

An in-vessel cryo-condensation pump is being designed for particle exhaust in the Advanced Divertor Configuration of the DIII-D tokamak. A schematic arrangement of this

* Research sponsored by the Office of Fusion Energy, U. S. Department of Energy, under contract DE-AC05-84OR21400 with Martin Marietta Energy Systems, Inc.

MASTER

Received by OCT

OCT 24 1990 *JMG*

DISTRIBUTION OF THIS DOCUMENT IS UNLIMITED

cryopump, located in the baffle chamber inside the DIII-D vacuum vessel, is shown in Fig.1. Monte Carlo calculations using the neutral particle transport code DEGAS¹ show that the outer shroud of such a pump will be exposed to energetic particle fluxes (reflected atomic particles that maintain a significant fraction of their original energy of a few tens of electron volts). Since, normally, these surfaces will be liquid nitrogen cooled, appreciable amounts of water vapor can condense over prolonged periods of pumping, even under high vacuum conditions. If this condensed layer of water vapor gets desorbed as a result of energetic particle impact, it can adversely affect the plasma performance and can potentially precipitate plasma disruption. Indeed, during experiments conducted in the PDX tokamak, when a liquid nitrogen cooled panel was positioned in the dome region of the device, numerous plasma disruptions were observed², and these disruptions are attributed to the desorption of water vapor due to the impingement of energetic particles from the plasma.

II. OBJECTIVE OF THE EXPERIMENT

Monte Carlo calculations show³ that in certain regions of the pump, energetic particle fluxes on the order of 10^{16} cm^{-2} at energies of about 10 eV are present. The spatial flux distribution of these particles, shown in Fig.2, is highly peaked at surfaces facing the baffle throat. The experiment described below is designed to simulate the effect of this energetic particle flux on water vapor cryo-condensate. This is done by exposing a liquid nitrogen cooled disk, on which a thin layer of water vapor is condensed, to a tenuous plasma formed by electron cyclotron heating (ECH). The object is to assess the seriousness of particle induced desorption from liquid nitrogen cooled surfaces of the pump, under conditions that are similar to that encountered by the DIII-D Advanced Divertor Cryopump.

III. EXPERIMENTAL DETAILS

The experiment was performed in an electron cyclotron resonance plasma device⁴ with plasma densities of 10^{10} - 10^{11} cm^{-3} and electron temperatures of 3-15 eV. The experimental arrangement is shown schematically in Fig.3. The hydrogen plasma is created by injecting approximately 500 W of microwave power at 2.45 GHz, in a single cell mirror arrangement⁴. Central densities of up to 10^{11} cm^{-3} and electron temperatures of up to 17.5 eV have been obtained. At the edge of the plasma (radius = 7 cm), a plasma density of about 2×10^{10} cm^{-3} and an electron temperature of about 3 eV have been measured⁵. At these parameters, the sheath potential, and hence the ion energy, is about 10 eV, and the ion arrival rate at the front of the disk is on the order of 10^{16} cm^{-2} . Thus, the particle flux incident on the surface of a disk located at the plasma edge is similar to the particle flux anticipated at the outer surfaces of the cryopump. A copper disk (1.25 cm thick and 5 cm diameter), that can be cooled to 77 K by circulating liquid nitrogen through the cooling channels around the disk, is located at the edge of the plasma. This disk serves as the cryo-condensing surface for water vapor with an estimated pumping speed of about 1000 l/s.

The plasma chamber is connected to another chamber through a 1 mm diameter aperture, and a residual gas analyzer (RGA) is located in this second chamber. This chamber equipped with the RGA is differentially pumped with a small turbo pump. The aperture provides the necessary pressure gradient between the main plasma chamber and the RGA.

IV. EXPERIMENTAL PROCEDURE

The pumping speed of the main pump was determined with the help of a standard air leak. The water vapor background with and without the ECH plasma in the main chamber was measured. The copper disk was then cooled by circulating liquid nitrogen through the cooling loops around the disk. Air was admitted to the main chamber through a constant leak of 5.0×10^{-2} torr l/s for 5 minutes. The copper disk, being an efficient cryo-condensation pump for water vapor, with a pumping speed of approximately 1000 l/s, collected a layer of water vapor on its surface. With the liquid nitrogen continuing to circulate, an ECH plasma is formed for 5 s duration and the water vapor peak during this discharge is monitored by the RGA. It must be mentioned at this point that, with zero magnetic field, and hence with no plasma, a 5 s ECH pulse did not produce any noticeable increase in the RGA water vapor signal. The discharge was repeated several times and the water vapor reading (peak corresponding to both H₂O and HO) was noted during each of these discharges. In order to understand the transport of particles from the main chamber to the RGA chamber, methane gas was introduced into the main chamber through a piezo electric valve, with and without the plasma and the RGA response was measured.

IV. DISCUSSION OF RESULTS

Fig. 4 shows the RGA signal corresponding to water vapor (the envelopes corresponding to H₂O and HO peaks) during the discharge duration. During subsequent discharges the amplitude of the signal is reduced progressively as shown in Fig.5.

Calibration with a standard leak showed the pumping speed, S_{air} , of the pump in the main chamber to be 124 l / s. Knowing this pumping speed and the pressure, p , during condensation, the air leak rate during condensation is calculated to be:

$$Q_{\text{air}} = S_{\text{air}} p = 124 \times 4.0 \times 10^{-4} = 5.0 \times 10^{-2} \text{ torr l / s}$$

The water vapor content in atmospheric air is quoted⁵ to be 1.57 % (the water vapor content varies in a wide range depending on the humidity and altitude. At sea level this variation⁶ is between 0.6 % - 3.8 %). Using the value from reference 5, the water vapor leak rate is estimated to be:

$$Q_{wv} = 5.0 \times 10^{-2} \times 0.0157 = 7.8 \times 10^{-4} \text{ torr l / s}$$

The pumping speed of the disk for water vapor, S_{wv} , assuming a sticking coefficient of unity for water vapor on a 77 K surface, is given by

$$S_{wv} = 3.64 (T/M)^{0.5} A,$$

where T is the temperature = 300 K, M is the molecular weight = 18, and A is the area of the 77 K surface in cm². In our case, substitution of the values gives

$$S_{wv} = 1000 \text{ l / s}$$

Thus the total water vapor condensed, N_c , for a condensation time, t_c , is given by

$$\begin{aligned} N_c &= Q_{wv} [S_{wv} / (S_{wv} + S_{air})] \times t_c \\ &= 0.21 \text{ torr l} \end{aligned}$$

Calibration of the RGA signal in terms of a desorption throughput can only be done in a crude manner. The transport of particles from the main chamber to the RGA, in the presence of the mirror plasma, is complicated. When water vapor in the form of steam was

puffed into the plasma through a piezo electric gas valve and the RGA response was observed, the results were not reproducible. This may be due to the peculiarities of water vapor as opposed to a gas. Therefore, methane gas was pulsed into the main plasma chamber with and without the plasma to understand the gas propagation from the plasma chamber to the RGA chamber. The results are shown in Figs. 6 and 7. The RGA signal for methane with the plasma is 0.32 V while the signal when the plasma is not present is about 1.9 V. Thus, for the same amount of gas feed, the signal without the plasma is about six times the signal with the plasma present. In the presence of the plasma, the methane gas is ionized, and transported along the field lines into the walls of the main chamber and to the mouth of the main pump, thereby effectively reducing the number of particles reaching the RGA chamber through the 1 mm diameter aperture. When there is no plasma, the throughput is decided by the molecular conductance of the aperture and the pressure gradient across it.

$$\text{the molecular conductance of the aperture} = 0.13 \text{ l/s}$$

During the methane injection, the pressure in the main chamber rose from 4×10^{-4} torr to 5×10^{-4} torr. The methane partial pressure in the main chamber is thus 1.0×10^{-4} torr. Thus the methane throughput to the RGA chamber is,

$$Q_m = 1.3 \times 10^{-5} \text{ torr l/s}$$

The RGA signal corresponding to this (fig.7) is 1.9 V. Since the pumping speed for methane in the main chamber is 124 l/s (assumed to be the same as measured for air), and the pressure is 1.0×10^{-4} torr,

The methane throughput to the main chamber = $1.24 \cdot 10^{-2}$ torr l / s

With plasma, the same throughput of methane produced an RGA signal of 0.32 V. We now assume the response by the RGA and the transport through the plasma by water vapor is similar to methane. Since the RGA signal for water vapor is about 0.15 V, it corresponds to about 6×10^{-3} torr l / s. Approximately 50 % of this pressure rise during discharge is due to desorption from the disk, the remainder coming from the vacuum wall. Thus a rough estimate for the desorption throughput from the disk is 3×10^{-3} torr l/s. Since the surface area of the disk is 20 cm^2 , the desorption rate is $\sim 10^{-4}$ torr l s⁻¹ cm⁻². While this desorption rate appears small, it becomes appreciable as the total area of the liquid nitrogen cooled surfaces of the cryopump is $\sim 10^5 \text{ cm}^2$. Thus energetic particle induced desorption of water vapor from cryogenic surfaces of the pump is a potential problem.

V. CRYOPUMP CONFIGURATION

The pump configuration that has evolved out of this study is shown in Fig.1. This arrangement minimizes the effects of energetic particles. This is accomplished by 1) directing the mouth of the pump away from the baffle chamber throat so that there is no direct line of sight on the cryogenic surfaces from the divertor strike region and, 2) introducing a shield (near room temperature) around the liquid nitrogen shroud that will intercept the bulk of the energetic particle flux. DEGAS calculations show that these changes will produce substantial decrease in the energetic particle flux impinging on the cryogenic surfaces while producing only a small decrease (<10 %) in the pumping speed.

VI. CONCLUSIONS

When a surface on which water vapor was cryogenically condensed (77 K) was exposed to

a tenuous plasma (density $\sim 10^{10} \text{ cm}^{-3}$, electron temperature $\sim 3 \text{ eV}$), significant desorption ($\sim 10^{-4} \text{ torr l s}^{-1} \text{ cm}^{-2}$) of the condensate occurred. This result suggests that cryogenic surfaces operating inside the tokamak vacuum, particularly the liquid nitrogen cooled surfaces on which water vapor can condense over prolonged periods of time, should be shielded from impingement of energetic particles emanating from the plasma.

ACKNOWLEDGEMENTS

Discussions with G. Jackson, A. Langhorn, A. Mahdavi, M. Schaffer, and H. Kugel are acknowledged. The authors also acknowledge the help received from Tom Rayburn in setting up the experiment.

DISCLAIMER

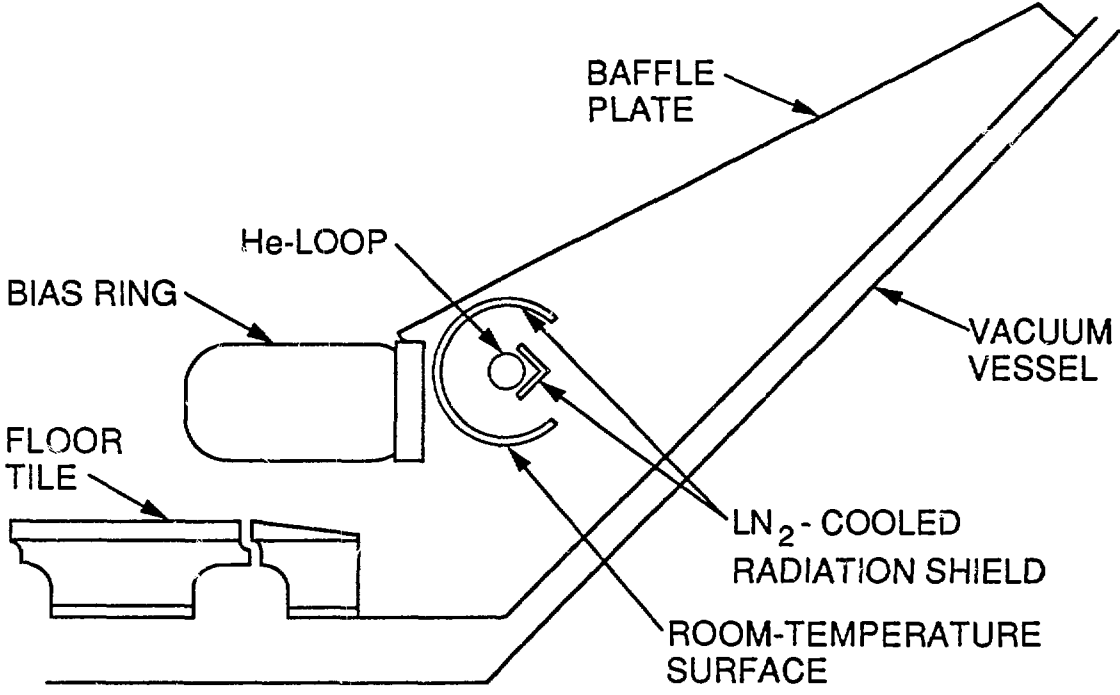
This report was prepared as an account of work sponsored by an agency of the United States Government. Neither the United States Government nor any agency thereof, nor any of their employees, makes any warranty, express or implied, or assumes any legal liability or responsibility for the accuracy, completeness, or usefulness of any information, apparatus, product, or process disclosed, or represents that its use would not infringe privately owned rights. Reference herein to any specific commercial product, process, or service by trade name, trademark, manufacturer, or otherwise does not necessarily constitute or imply its endorsement, recommendation, or favoring by the United States Government or any agency thereof. The views and opinions of authors expressed herein do not necessarily state or reflect those of the United States Government or any agency thereof.

REFERENCES

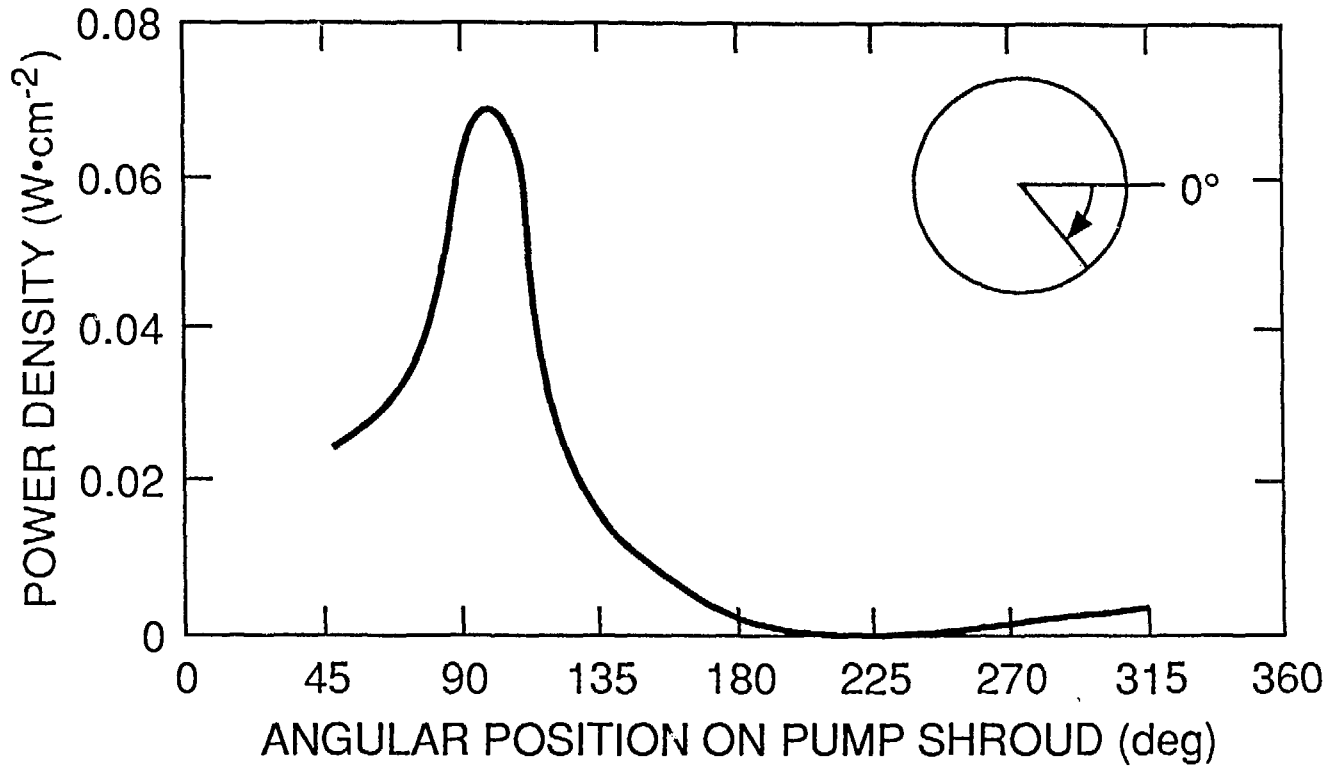
- 1.D. Heifetz et al., J. Comp. Phys., 42, 309 (1982)
2. Kingston Owens, Princeton Plasma Physics Laboratory, Private Communication
3. L. W. Owens, unpublished
4. T. Uckan, Rev. Sci. Instrum., 58, 17 (1987)
- 5.A. Roth, Vacuum Technology,pp.4, Noth-Holland, 1982

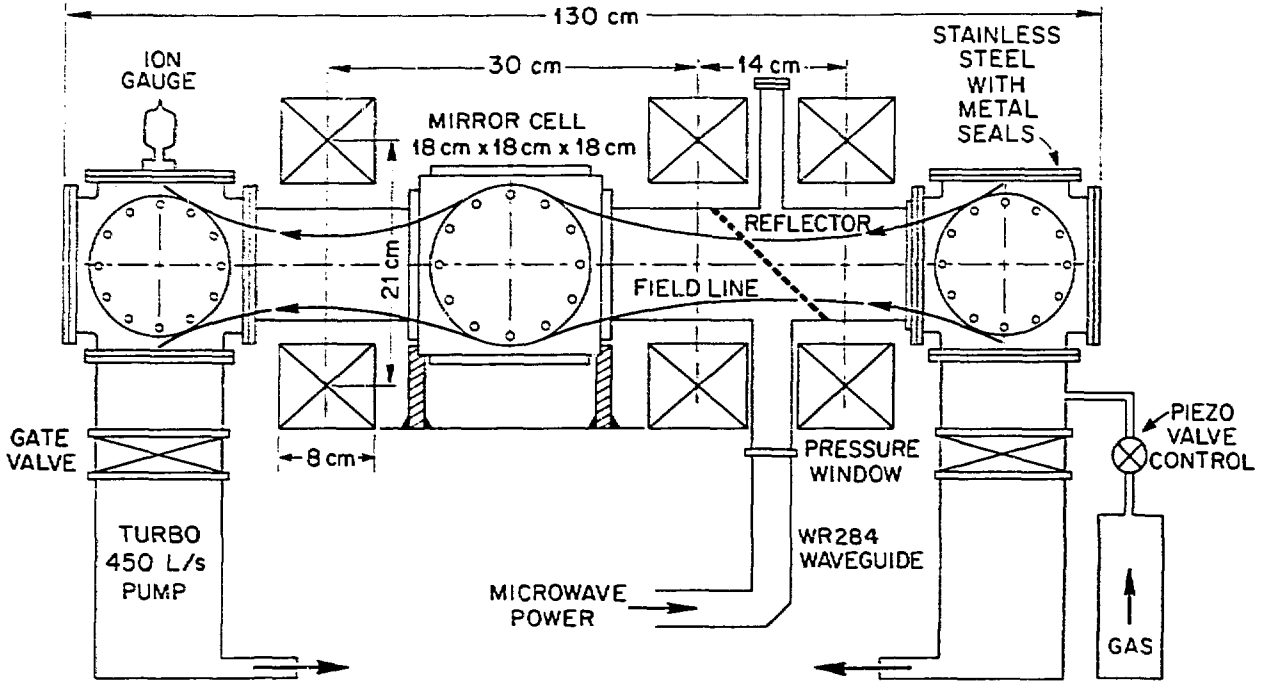
FIGURE CAPTIONS

- fig.1: A schematic arrangement of the pump, located inside the baffle chamber of the DIII-D tokamak
- fig.2: Energetic particle power flux distribution on the outer surface of the pump. The orientation corresponding to zero degree is shown in Fig.1
- fig.3: The plasma facility. The cryogenic disc was mounted at the middle, on the side flange of the mirror cell.
- fig.4: The oscillogram showing the envelopes of the mass 18 and mass 17 peaks (H_2O & HO) in the RGA during the plasma discharge.
- fig.5: The variation in the RGA signal with number of discharges
- fig.6: The envelopes of peaks corresponding to mass 16,15, and 14 during a methane pulse into the ECH plasma
- fig.7: The envelopes of mass 16, 15, and 14 during a similar methane pulse without the plasma being present.



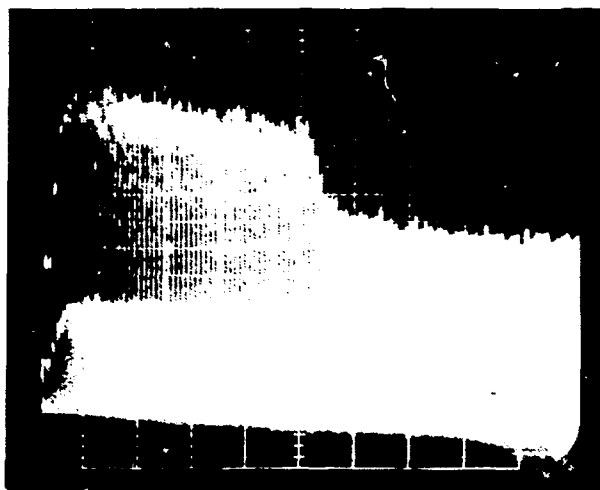
ORNL-DWG 90M-2955 FED



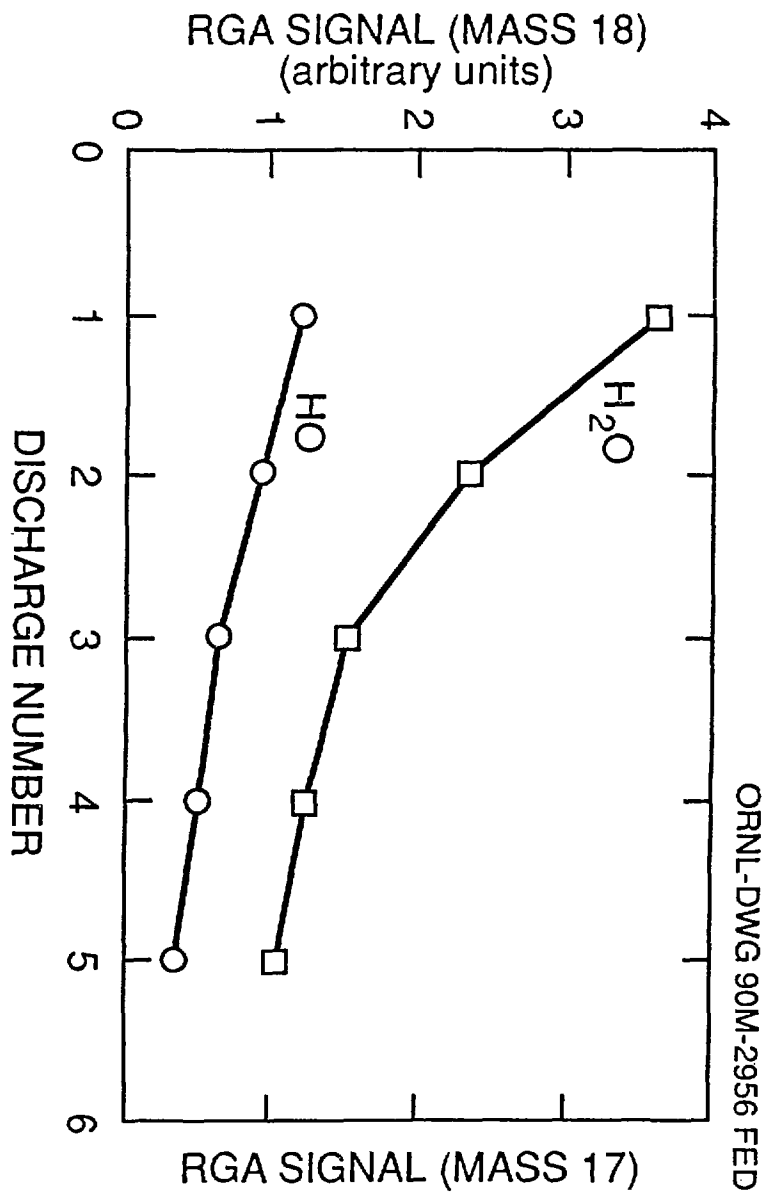


ORNL-PHOTO 6184-90 FED

50 mV/div



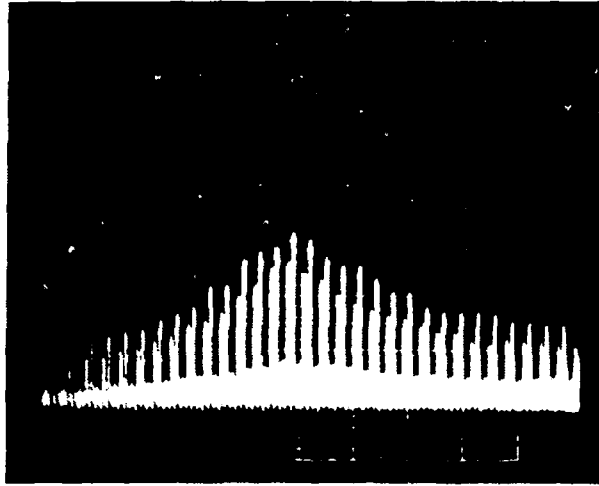
1 s/div



ORNL-DWG 90M-2956 FED

ORNL-PHOTO 6182-90 FED

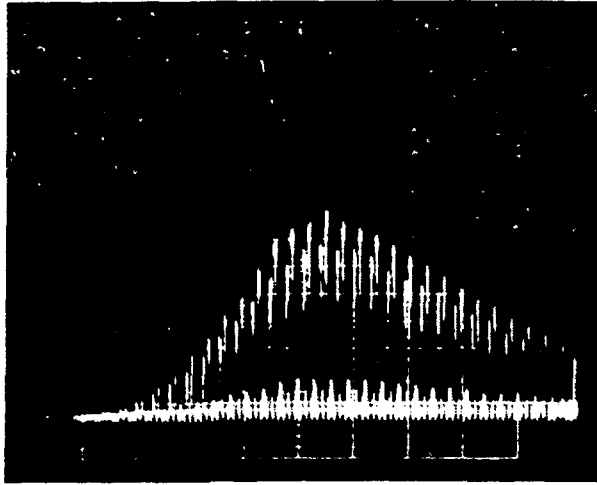
0.1 V/div



0.1 s/div

ORNL-PHOTO 6183-90 FED

0.5 V/div



0.1 s/div